Advances in Automobile Engineering
ISSN: 2167-7670

Al-Saadi et al., Adv Automob Eng 2016, 5:1
DOI: 10.4172/2167-7670.1000134

Research Article Open Access

Simulations of Aerodynamic Behaviour of a Super Utility Vehicle Using Computational Fluid Dynamics

Ahmed Al-Saadi*, Ali Hassanpour and Tariq Mahmud

School of Chemical and Process Engineering, University of Leeds, Woodhouse Lane, Leeds, UK

Abstract

The main objective of this study is to investigate ways to reduce the aerodynamic drag coefficient and to increase the stability of full-size road vehicles using three dimensional Computational Fluid Dynamics (CFD) simulations. The baseline model of the vehicle used in the simulation is the Land Rover Discovery. There are many modern aerodynamic add-on devices which are investigated in this research. All of these devices are used individually or in combination. These add-on devices should not affect the vehicle capacity and comfort. In this study three velocities of the air is used: 28 m/s (100.8 km/hr), 34 m/s (122.4 km/hr) and 40 m/s (144 km/hr). The calculated drag coefficient for the baseline model of Land Rover Discovery agrees very well with the experimental data. It is clear that the use of a ventilation duct has a significant effect in reducing the aerodynamic drag coefficient.

Keywords: Aerodynamics; Turbulence; Computational methods

Introduction

A steady increase in global energy demand has a direct influence on the fuel prices. This together with the environmental problems caused by the exhaust gases of cars is the main motives behind needs to reduce fuel consumption of road vehicles. Reducing aerodynamic drag can lead to a reduction in fuel consumption leading to less environment problems. Control of global warming has put massive pressure on designers to improve the current designs of vehicles using minimal changes in the shape [1]. A good example is wagon car (square back) which has a relative high rake angle (ϕ) causing the flow separation just at the roof end before the rear windscreen. If the flow would remain attached, it could create a strong downwash of the flow field which causing a high degree of turbulence in the wake and this would increase the drag. A high rake angle decreases the downwash and the induced drag, but will on the other hand have a negative impact on the pressure drag [2].

The simple wagon car model was achieved with modifications of front surfaces by Guo et al. [3] using CFD analysis by the K-ε turbulence model. The bottom of the saloon car body was assumed as a flat surface. The wheels, wind gaps and rear view mirrors were neglected in modelling using finite element model to simplify the solution. This analysis was based on three different slantwise angles of the back windshield, i.e. β=17°, β=23° and β=30°. Barbut and Negrus [4] studied the influence of the lower part design of sedan cars on the air resistance. Redesign of the lower part of the sedan car could reduce the aerodynamic drag equivalent to approximately 20%.

Computational Fluid Dynamic (CFD) using the parallel version of DxUNSp code was used to optimize the design of the lower part of the sedan car. Song et al. [5] optimized external design of a sedan car by using the Artificial Neural Network method. The authors focused on modifying the rear external design of the sedan car by using a modification of the trunk, the rear side, and the rear undercover to optimize the rear shape of the YF SONATA model. The realizable K-ε model-based Detached Eddy Simulation model was used because of its accuracy and generating comparable results to the experimental data. Koike et al. [6] used vortex generators in the saloon car to reduce air resistance. Vortex generators were used to minimize the separation of flow near the vehicle's rear end. They create drag, but also reduce drag by preventing flow separation at downstream. Hu and Wong [7] studied the effect of the spoiler on the sedan car by numerical simulations using the standard k-ε model to simulate the aerodynamic of the simplified three dimensional Camry model. Kang, et al. [8] studied reduction in the aerodynamic drag of the saloon car using a movable arc-shaped semi-diffuser device which was installed on the rear bumper of the sedan.

The advantage of this device is that it disappears under the rear bumper, but it reappears only at high speeds (70 km/hr ~ 160 km/hr). Raju and Reddy [9] added the device in the rear part of the car to reduce the air resistance and that led to a reduction in the fuel consumption. This attachment was moved into outer or inner sections depend on the conditions for controlling the pressure difference. The hydraulic system was used to control the movement of this attachment which was under the control of the driver. Sivaraj and Raj [10] used the base bleed to improve the aerodynamic drag by using ANSYS Fluent software. The suggested modification led to a decrease in the fuel consumption, more stability on the road and also minimization of dangerous interactions with other cars on the road.

Most of the previous CFD simulations are based on simple geometries, except the studies carried out by Levin and Rigdal [2] and Song et al. [5] which were relevant to actual vehicle geometries. Levin and Rigdal [2] studied the differences of aerodynamic behaviour between sedan and wagon cars. Song et al. [5] modified the rear external design of a sedan car (YF SONATA model) including the trunk, rear side, and rear undercover to optimize the rear shape of the car. Further, Koike et al. [6] used vortex generators in a saloon car to reduce air resistance. Hu and Wong [7] studied the effect of the airfoil spoiler and plate spoiler on a sedan car. Kang, et al. [8] used a movable arc-

***Corresponding author:** Ahmed Al-Saadi, School of Chemical and Process Engineering, University of Leeds, Woodhouse Lane, Leeds, UK, Tel: +44 113 243 1751; E-mail: pmaash@leeds.ac.uk

Received March 24, 2016; **Accepted** March 31, 2016; **Published** April 02, 2016

Citation: Al-Saadi A, Hassanpour A, Mahmud T (2016) Simulations of Aerodynamic Behaviour of a Super Utility Vehicle Using Computational Fluid Dynamics. Adv Automob Eng 5: 134 doi:10.4172/2167-7670.1000134

shaped semi-diffuser device which was installed on the rear bumper of a sedan car to reduce the aerodynamic drag of the car. Raju and Reddy [9] added a device (collapsible wind friction reduction) in the rear part of the car to reduce the air resistance. Sivaraj and Raj [9] used the base bleed to improve the aerodynamic drag.

These researchers focused on either drag or lift. Therefore, the overall objective of this study is to improve the performance of road vehicles by reducing the fuel consumption through the reduction of drag forces and increasing their stability on the road via an increase of pressure over the car by modifications to the vehicle aerodynamics. Land Rover Discovery is used as a model vehicle for this investigation. CFD simulations were carried out using ANSYS Fluent 16.0 software. Computed drag coefficient for the baseline model of Land Rover Discovery (The official Media Centre for Jaguar Land Rover, 2012 [11]) agrees very well with the experimental data. Modifications of the external shape and aerodynamic add-on devices (such as ventilation duct and ditch on the roof) are used to improve the aerodynamic behaviour of this car. These add-on devices do not affect the vehicles capacity and comfort.

Methodology for the CFD Simulation Analysis

All computational models of the Land Rover Discovery, which includes baseline and modifications, are prepared in SolidWorks 2014 software and the CFD simulations are performed with the ANSYS Fluent 16.0 software. The dimensions of Land Rover Discovery model (The official Media Centre for Jaguar Land Rover, 2012) are: overall length of 4.835 m, overall height of 1.887 m, width without side mirrors of 1.915 m, and the wheelbase of 2.510 m. (Figure 1) illustrates the baseline external design of the Land Rover Discovery with coordinate directions. (Figure 2) shows the computational domain with dimensions in which the whole geometry of car is placed. To avoid the possible wall boundary layer effect, the cross-sectional area of the computational domain is set larger than the wind tunnel. Meshing of the computational domain is a very crucial step in design analysis. To reduce the calculations time one-half of the computational domain and the geometry of the car is used. ANSYS Fluent was used for mesh generation with varying levels of refinement. Optimization of mesh parameters was carried out by analysis the mesh data. Unstructured tetrahedral cells were used throughout the global domain to cope with the geometrical complexity of the model car as shown in (Figure 3). Eighteen types of mesh (for details see (Table 1) were tested to check the best global mesh. Different mesh types and sizes as well as three eddy-viscosity based turbulence models are investigated. In order to generate refined mesh to represent the model car geometry accurately, the computational domain was divided into two zones. A refined zone, referred to as the Control Volume Box (CVB) was used around the car with five meshes and the rest of the computational domain with the global mesh. This mesh arrangement is illustrated in (Figure 4). Further mesh refinement was carried out by using three CVBs as shown in (Figure 5). Inflation layers with prismatic cells were used to provide an accurate estimation of the velocity profiles near the surfaces of the car. The prismatic growth ratio for each layer is 1.2. Ten types of inflation layers were tested to find an optimum number of inflation layers as shown in (Table 2).

Three CVBs with five layers of inflation was adopted for simulations as depicted in (Figure 6). The number of elements in the computational domain can affect the result of the computation analysis. After an extensive testing of the number of elements, a mesh of approximately 14.1×10^6 elements was chosen as the standard level of the grid fineness in terms of accuracy and computational time. The maximum Skewness of standard mesh was 0.897066 and the minimum Orthogonal Quality was 0.012722. For this study, the following conditions were applied: uniform inlet velocity of 28 m/s (100.8 km/hr), 34 m/s (122.4 km/hr) and 40 m/s (144 km/hr) from the frontal side of the car model.

Two types of wall boundary conditions were used: (i) stationary walls with no slip (ii) the outside walls of computational domain were symmetric and that means they have no viscous effect on the analysis. Three turbulence models are used in this study: realizable k–ε, standard k-ω and shear stress transport k-ω. The drag (CD) and lift (CL) coefficients were calculated based on the following equations in this study: where FD is the drag force (N), FL is the lift force (N), ρ is the air density (kg/m^3), V is the initial air velocity (m/s), A is the frontal cross sectional area of the vehicle (m^2).

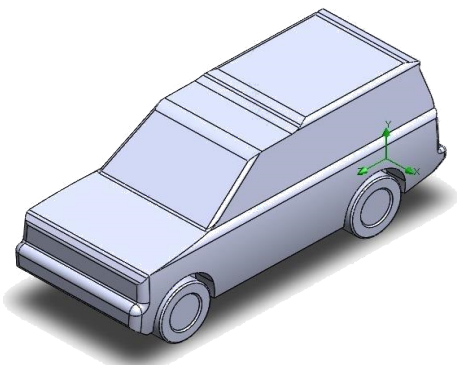

Figure 1: The baseline external design of the Land Rover Discovery.

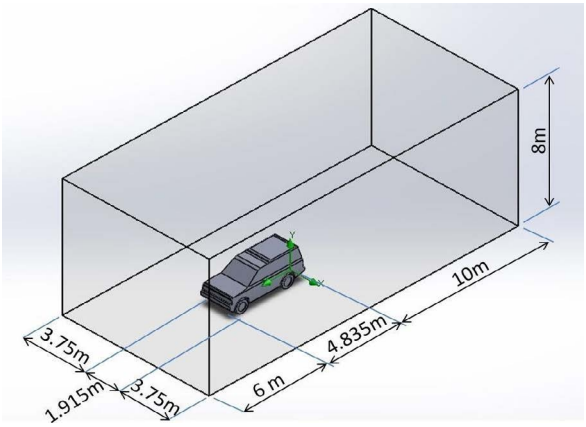

Figure 2: Computational domain with dimensions.

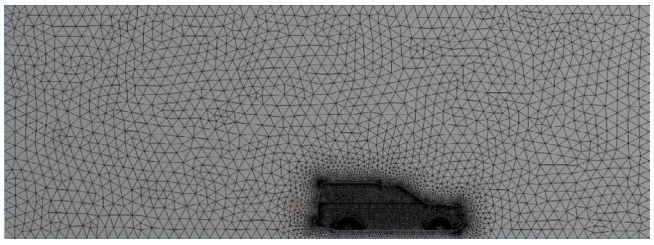

Figure 3: Unstructured tetrahedral global mesh.

Relevance center	Size function	Nodes	Elements	Maximum Skewness	Minimum Orthogonal Quality
Coarse (Default)	Proximity and curvature	1,35,169	7,24,818	0.84243	0.22021
Coarse (Modify)	Proximity and curvature	4,87,106	26,41,923	0.90896	0.14019
Coarse (Default)	Curvature	1,18,803	6,39,082	0.86293	0.25967
Coarse (Modify)	Curvature	4,47,432	24,33,631	0.88695	0.14164
Coarse (Default)	Proximity	75,585	4,01,510	0.91503	0.18784
Coarse (Modify)	Proximity	2,60,524	14,13,863	0.91182	0.1328
Medium (Default)	Proximity and curvature	2,36,507	12,72,217	0.88784	0.18591
Medium (Modify)	Proximity and curvature	4,97,144	26,96,470	0.90334	0.13398
Medium (Default)	Curvature	2,15,830	11,62,337	0.86304	0.20812
Medium (Modify)	Curvature	4,47,432	24,33,631	0.88695	0.14164
Medium (Default)	Proximity	1,68,900	9,03,978	0.90677	0.16638
Medium (Modify)	Proximity	2,60,525	14,13,805	0.91182	0.1325
Fine (Default)	Proximity and curvature	2,53,775	13,59,787	0.89641	0.13824
Fine (Modify)	**Proximity and curvature**	**5,11,826**	**27,76,114**	**0.93597**	**0.1367**
Fine (Default)	Curvature	2,27,727	12,21,294	0.88792	0.1321
Fine (Modify)	Curvature	4,47,432	24,33,631	0.88695	0.14164
Fine (Default)	Proximity	1,15,209	6,09,235	0.93302	0.13914
Fine (Modify)	Proximity	2,52,205	13,69,012	0.89017	0.22941

Table 1: Eighteen types of global mesh.

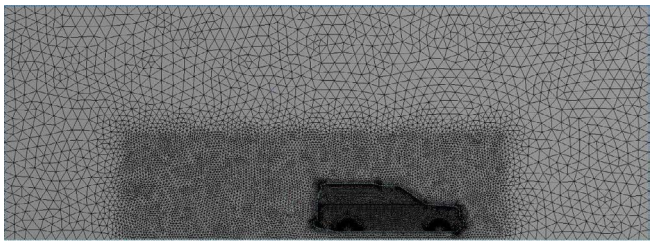

Figure 4: Mesh with one control volume box.

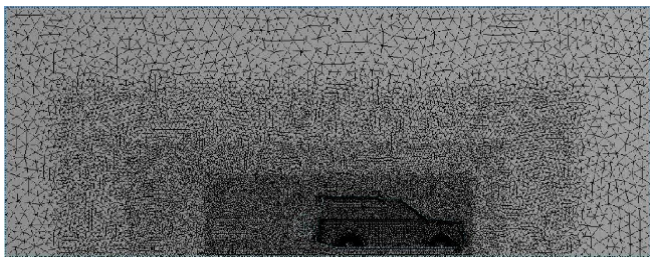

Figure 5: Mesh with three control volume boxes.

Validation of CFD Analysis

The full scale model described above was simulated using the ANSYS Fluent 16.0. The drag coefficient obtained from the ANSYS Fluent for the baseline model was validated with experimental data from the website of the Land Rover Company (The official Media Centre for Jaguar Land Rover, 2012 [11]) as shown in (Table 3). Realizable k–ε is suitable for external flows around complex geometries and good for shear layers. This model solves for kinetic energy (k) and turbulent dissipation (ε).

The Modification Models

Various models for reducing air resistance based on a completely new design as well as modifications to previous suggested models have been proposed in this study. (Figure 7) shows the longitudinal duct that is used in Land Rover Discovery model as a modification to improve the aerodynamic behavior. This technique leads to a reduction in the drag aerodynamic and vortices behind the car in addition to cooling the engine and other facilities. The ditch on the roof is used to improve the aerodynamic behaviour for this model as shown in (Figure 8). These modifications generates a lower drag force than baseline model,

Inflation Algorithm	No. of layers	Elements	Maximum Skewness	Minimum Orthogonal Quality
Pre	1	3,415,186	0.925	0.019824
Pre	2	3,524,345	0.925	0.019274
Pre	3	3,637,365	0.925	0.015432
Pre	4	3,761,233	0.925	0.013537
Pre	**5**	**3,877,815**	**0.925**	**0.011468**
Pre	6	3,979,709	0.925	0.009568
Pre	7	4,039,489	0.925	0.0088265
Pre	8	4,126,702	0.925	0.0087753
Pre	9	4,291,486	0.925	0.0081368
Pre	10	4,504,357	0.925	0.0071845

Table 2: Mesh refinement with inflation layers.

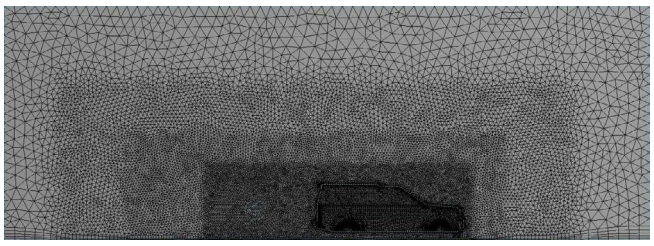

Figure 6: Mesh with five inflation layers around the car and over the road.

Baseline Model (Real Model) *	ANSYS Fluent results		
	Realizable k–ε	Standard K-ω	Shear stress transport K-ω
Cd=0.4	CD= 0.400146	CD= 0.40546	CD= 0.41998
Mean Absolute Percentage Error	0.0365%	1.365%	4.995%
* The official Media Centre for Jaguar Land Rover, 2012.			

Table 3: Validation of numerical results.

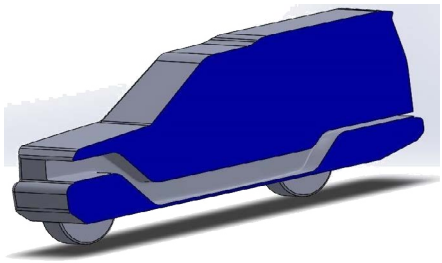

Figure 7: Cross sectional area shows the longitudinal duct in ISO view.

but it is difficult to add duct and ditch on the roof of the car to the baseline model.

Results

The streamline around the baseline of the Land Rover Discovery is shown in (Figure 9). Two main problems appeared with this design: vortices behind the car and high velocity of air above the front of the roof. The new external design of the Land Rover Discovery with all modifications generates a lower drag force than baseline model, but it is difficult to add duct and ditch on the roof of the car. (Figure 10) shows the pressure distribution on the body surface of the baseline model. There are also pressure related problems with this design: low pressure above the car especially at the front of the roof, high pressure in front of the car especially on the front member of the car, low pressure behind the car. Summary of the results is shown in (Tables 4 and 5). (Table 4) shows the effect of the velocity on the drag force and lift force (depending on the realizable k–ε turbulence model). Drag and lift forces have increased with increasing the velocity of the air. (Table 5) illustrates the drag coefficient and lift for many models of car. Realizable k–ε and standard K-ω turbulence models are more accurate than shear stress transport K-ω in this case of study.

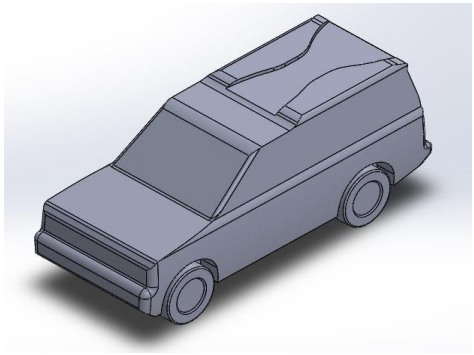

Figure 8: Land Rover Discovery model with ditch on the roof.

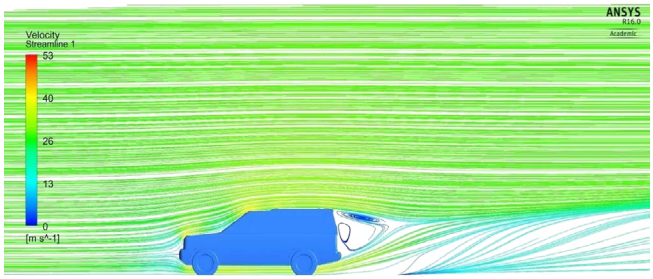

Figure 9: Streamline around the baseline of Land Rover Discovery.

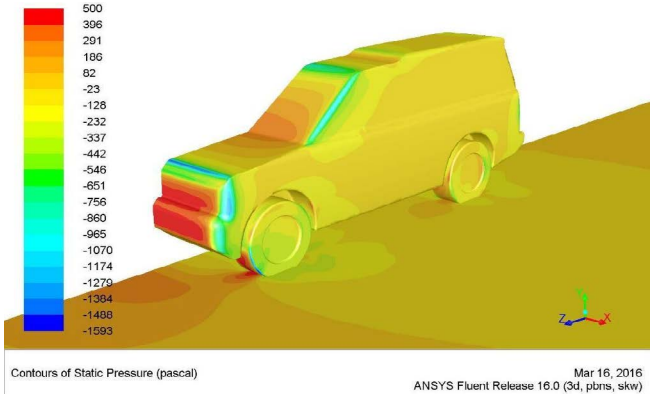

Figure 10: Contours of pressure for the baseline of the Land Rover Discovery.

	Velocity (m/s)	Base Line Model		Car Model with Duct		Car Model with Duct	
		Drag Force (N)	Lift Force (N)	Drag force (N)	Lift Force (N)	Drag Force (N)	Lift Force (N)
1	28	576.45	123.21	517.37	134.55	575.73	47.82
2	34	849.97	181.82	762.87	198.39	848.91	70.52
3	40	1176.43	251.66	1055.87	274.59	1174.97	97.60

Table 4: The effect of the velocity on the drag force and lift force (Realizable k–ε).

	Base Line Model		Car Model with Duct		Car Model with Ditch	
	Realizable k- ε	Standard k- ω	Realizable k- ε	Standard k- ω	Realizable k- ε	Standard k- ω
CD	0.400146	0.40546	0.36201	0.39965	0.39965	0.39984
CL	0.0856	0.0858	0.0934	0.0971	0.0332	0.0349

Table 5: The drag coefficient and lift for many models of car.

Conclusion

Most properties of the fluid flow vary behind the car, so we need to increase the length of the computational domain behind the car. Use three volume control boxes in the computational domain to capture all the properties around the car. The optimal technique found to be used in mesh is the fine relevance center and proximity and curvature interims of size function with other advanced settings. Regards inflation (number of mesh layers around the car body) the optimum number of layers found to be 5. Realizable k–ε and standard K-ω turbulence models are more accurate than shear stress transport K-ω in this case of study. The duct technique was used in the vehicle studies in this work because the use of the duct increases the pressure behind the car and decreases the pressure at the front of the car. The ditch on the roof of the car increased the pressure above the car and this leads to an increase in the road stability of the vehicle, especially at high speeds.

Acknowledgments

The authors dedicated their thanks to all who participated in this research, especially the Ministry of Higher Education and Scientific Research (MOHESR) in Iraq and also Al-Qadisiya University in Iraq for sponsoring the first author.

References

1. Krishnani PN (2009) CFD study of drag reduction of a generic sport utility vehicle. Doctoral dissertation, American Society of Mechanical Engineers.
2. Levin J, Rigdal R (2011) Aerodynamic analysis of drag reduction devices on the underbody for SAAB 9-3 by using CFD. Master's thesis, Chalmers Univesity of Technology, Goteborg, Sweden.
3. Guo LX, Zhang YM, Shen WJ (2011) Simulation analysis of aerodynamics characteristics of different two-dimensional automobile shapes. Journal of Computers 6: 999-1005.
4. Barbut D, Negrus EM (2011) CFD analysis for road vehicles-case study. Incas Bulletin 3: 15-22.
5. Song KS, Kang SO, Jun SO, Park HI, et al. (2012) Aerodynamic design optimization of rear body shapes of a sedan for drag reduction. International Journal of Automotive Technology 13: 905-914.
6. Koike M, Nagayoshi T, Hamamoto N (2004) Research on aerodynamic drag reduction by vortex generators. Mitshubishi Motors Technical Review.
7. Hu X, Wong TT (2011) A numerical study on rear-spoiler of passenger vehicle.

International Journal of Mechanical, Aerospace, Industrial, Mechatronic and Manufacturing Engineering 5: 1800-1805.

8. Kang SO, Jun SO, Park HI, Song KS, Kee JD, et al. (2012) Actively translating a rear diffuser device for the aerodynamic drag reduction of a passenger car. International Journal of Automotive Technology 13: 583-592.

9. Raju DKM, Reddy GJ (2012) A conceptual design of wind friction reduction attachments to the rear portion of a car for better fuel economy at high speeds. International Journal of Engineering Science and Technology 4: 2366-2372.

10. Sivaraj G, Raj MG (2012) Optimum way to increase the fuel efficiency of the car using base bleed. International Journal of Modern Engineering Research (IJMER). 2: 1189-1194.

11. The official Media Centre for Jaguar Land Rover (2012).